

Granular surface waves in a vibratory conveyor

A. Götzendorfer, C. A. Kruelle & I. Rehberg
Experimentalphysik V, Universität Bayreuth, Germany

ABSTRACT: We study the behaviour of dry granular material on vibratory conveyors. In our experiment we superpose a vertical vibration and a horizontal vibration of equal amplitudes and a phase shift of $\pi/2$. That means that every point of the support follows a circular trajectory. Standing waves oscillating at half the forcing frequency are observed within a certain range of the driving acceleration. The dominant wavelength of the pattern is measured for various forcing frequencies at constant amplitude. These waves are not stationary, but drift with a velocity equal to the transport velocity of the granular material, determined by means of a tracer particle.

1 INTRODUCTION

Providing a granular material with energy can make it behave like a liquid. One example are avalanches. The energy that particles gain when sliding down a steep slope leads to the fluidisation of large parts of the granular surface. Another example are surface waves in vibrated beds. When a layer of granular material is repeatedly kicked by an oscillating support, surface waves are excited that resemble Faraday waves known from thin layers of shaken liquids. The mechanism responsible for this granular pattern formation is not yet fully clear. What complicates the situation is that the type of the wave is probably not the same throughout the whole range of driving parameters and particle sizes over which the phenomenon has been observed. Metcalf et al. (1997) and Umbanhowar & Swinney (2000) pointed out that at low driving frequencies small particles travel half a wavelength during each forcing cycle, and patterns result from a sloshing back and forth motion of the granular material. In contrast, for high forcing frequency and big particles the movement of the individual grains is reported to be more random in character, and the horizontal mobility is estimated to be very low. Then one deals either with bending waves or density waves. It will be demonstrated in the next section that the experiments presented here concern the latter regime.

Clément et al. (1996) and Wassgren et al. (1997) investigated granular surface waves in vertically oscillated 2D or quasi 2D beds in rectangular containers. Pattern formation in cylindrical containers upon vertical oscillation was examined by Melo et al. (1994, 1995), Umbanhowar & Swinney (2000) and Metcalf et al. (1997). Our experiments differ from the above mentioned by the ring shaped geometry of

the container and an additional horizontal shaking component. The cited 2D and quasi 2D experiments work with containers that have a relatively low bed height/container length ratio of about 10 to 15. When filled up until the number of particle layers is comparable to that present in the experiments reported in this paper only very few waves fit into these boxes. In contrast, the circumference of our annular container is 130 times bigger than the bed height. This is enough to accommodate 27 waves of the longest observed wavelength. When driving parameters are such that the wavelength is shortest more than 60 waves are counted in the ring.

In industry machines like this are called vibratory conveyors. They are utilised to carry small components, coal pieces, cereal grains, fertilizer granulates, sands, powders, and so on. Transport results from the reflection symmetry breaking oscillation of the conveying trough.

2 EXPERIMENT

Our container consists of a ring-shaped trough, 5 cm wide and 141 cm in circumference (see Figure 1). For the experiments presented in this paper we used 466,000 spherical glass beads with a diameter of 1.11 ± 0.04 mm. In a close packing this number of particles would result in a filling height of 11.0 mm or 13.4 particle layers above the trough bottom. The container oscillates sinusoidally in the vertical direction. Additionally, the ring performs an angular oscillation around its axis of symmetry. The phase difference between these two vibration components is fixed at $\pi/2$ and the amplitudes are such that every point of the trough bottom follows a circular trajectory. The shaking amplitude was kept constant at $a = 1.47$ mm, with

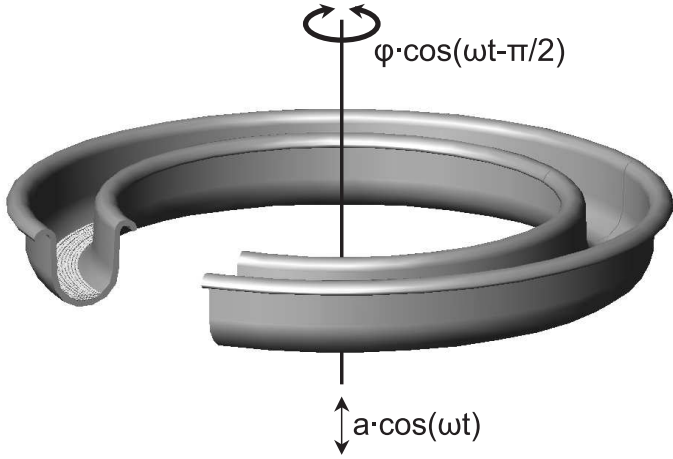


Figure 1. Geometry of the ring shaped container and its movement. An angular and a vertical vibration are superposed with a phase shift of $\pi/2$.

a standard deviation of 0.03 mm or 2%. A detailed description of the apparatus and the driving mechanism can be found elsewhere (Grochowski et al. 2004; Rouijaa et al. 2005). The illumination consists of 18 goose neck glass fibre light guides connected to 6 cold light sources. To visualize surface undulations the granulate is lighted under small angle. In a top view, peaks will then shine brightly, while valleys lie in the dark. Images are taken with a Kodak Ektapro high speed digital imaging system with a resolution of 239×192 pixel at rates of up to 1000 images per second.

3 RESULTS AND DISCUSSION

From earlier research into the transport properties of granular material upon circular shaking (Grochowski et al. 2004) it is known that the most important forcing parameter is the normalized maximum acceleration $\Gamma = a\omega^2/g$, where ω is the angular driving frequency and g the gravitational acceleration. We find standing surface waves oscillating at half the driving frequency in the range $20 \text{ Hz} < f < 29 \text{ Hz}$. Using measured values for the driving amplitude the corresponding acceleration Γ is calculated to lie in the interval $2.4 < \Gamma < 4.8$. At Γ below 2.4 the granular surface is flat. This is also true for Γ above 4.8, but here the layer flight time exceeds the forcing period, and kink type defects appear between regions oscillating out of phase.

Figure 2 shows a series of close-ups of the granular surface at $\Gamma = 3.0$. We analyse the evolution of the surface wave during a forcing cycle with the help of films taken at 1000 frames per second. The wave amplitude is highest after the support has passed its lowest position and accelerates upward. Then the wave amplitude decays, and the surface becomes eventually completely flat, when the container has passed its maximum position and accelerates downward. In the following half cycle, a wave builds up again with peaks at positions where before were valleys and vice versa. Its amplitude grows until it reaches a maximum

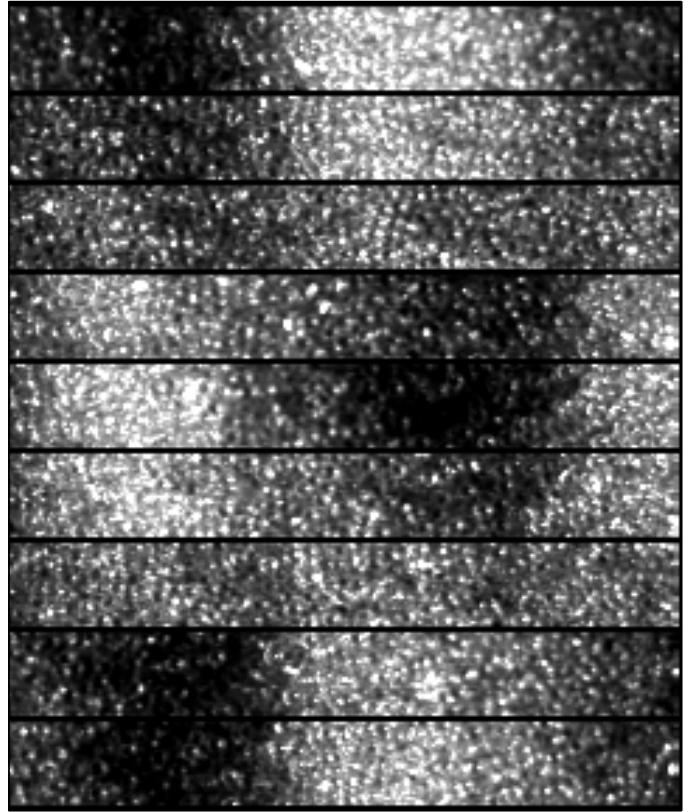


Figure 2. Close-up snapshots of the surface of the granular layer at a peak forcing acceleration $\Gamma = 3.00$. Time increases from top to bottom by 12ms between successive images. The length of the filmed section is 3.3 cm.

and the cycle starts anew.

In order to monitor the pattern dynamics, images are taken only once per forcing cycle, when the wave is at maximum amplitude. The fact that the waves are always oriented perpendicular to the side walls reduces the pattern to one dimension. We therefore evaluate the brightness along the circumference of the ring by averaging over the width of the trough. The ring circumference is subdivided into bins of 1.4 mm length. In order to reduce effects of inhomogeneous illumination, for all images and each bin its time average is subtracted. Short wavelength fluctuations are eliminated by the application of a Gaussian filter (see Jähne 2002) with a standard deviation of 2.3 bins. A search for extrema yields the peak and valley positions of the surface wave. The probability distribution function of the distances between neighbouring extrema shows a strong peak at the dominant wavelength. This analysis in real space is favoured over an evaluation in Fourier space, since it is more robust with respect to local perturbations of the wave pattern.

Figure 3 is a plot of the measured wavelength as a function of acceleration Γ . The wavelength of the surface wave decreases from 5.2 cm at onset to 2.3 cm just before it vanishes. Assuming a power law dependence, and allowing for a cutoff at a minimum wavelength λ_{\min} we fit a function of the form

$$\lambda = \lambda_{\min} + c \cdot \Gamma^p.$$

to the data. The best fit is drawn as a solid line in Figure 3. For the minimum wavelength λ_{\min} we obtain

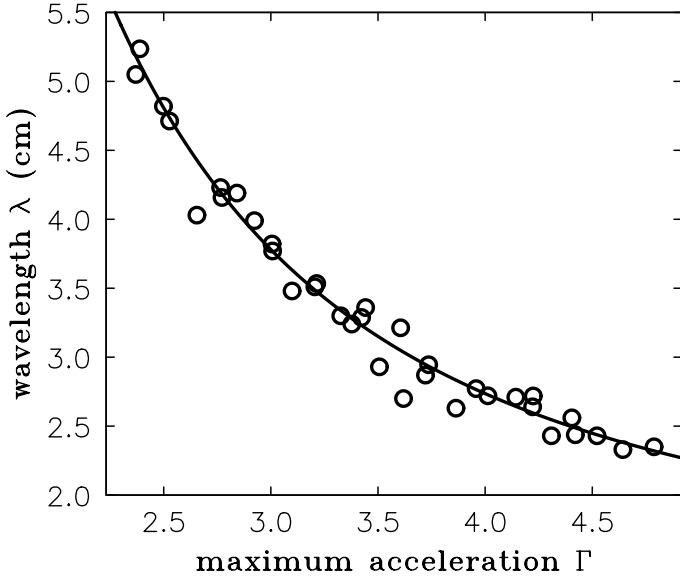


Figure 3. Circles represent the measured wavelength λ plotted over the normalized acceleration Γ . Throughout the measurement the driving amplitude was kept constant at 1.47 mm. The solid line is the graph of the function $\lambda = 1.3 \text{ cm} + 20 \text{ cm} \cdot \Gamma^{-1.9}$, the best fit to the data.

a value of $1.3 \pm 0.3 \text{ cm}$, which is approximately the depth of the granular layer. The values for the other parameters are $c = 20 \pm 4 \text{ cm}$ and $p = -1.9 \pm 0.3$.

How does this result compare to other published wavelength measurements? Umbanhowar & Swinney (2000) gave the most accurate formula describing the dispersion relation at constant acceleration $\Gamma = 3.0$ and low frequencies. It reads

$$\lambda/h = 1.0 + 1.1 \cdot \left(f \sqrt{h/g} \right)^{-1.32},$$

where h is the filling height assuming a filling fraction of 58%. Metcalf et al. (1997) additionally examined the dependence of the wavelength on the peak acceleration Γ at constant frequency. At low frequencies they found a slow rise in wavelength as the peak acceleration increases. The situation is completely different at high frequencies, where a sharp drop of the wavelength for increasing Γ has been reported. Furthermore at fixed peak acceleration the wavelength depends only weakly upon frequency, if at all. The crossover between the low and high frequency regimes occurs when the peak container velocity $v = 2\pi f a$ passes the critical value $v_{\text{gm}} \approx 3\sqrt{dg}$. Both Umbanhowar & Swinney (2000), and Metcalf et al. (1997) associated this crossover with a change in grain mobility. They noticed that for $v > v_{\text{gm}}$ the whole granular material performs a horizontal sloshing motion, while for $v < v_{\text{gm}}$ grains are essentially immobile in the horizontal direction. Note that

$$v < v_{\text{gm}} \Leftrightarrow f < 3/(2\pi a)\sqrt{dg} \Leftrightarrow f > \Gamma/(6\pi)\sqrt{g/d}.$$

This means that in measurements where Γ is kept constant the immobile grain regime is situated at high frequencies, whereas in the experiments presented in this paper the same behaviour is expected below the

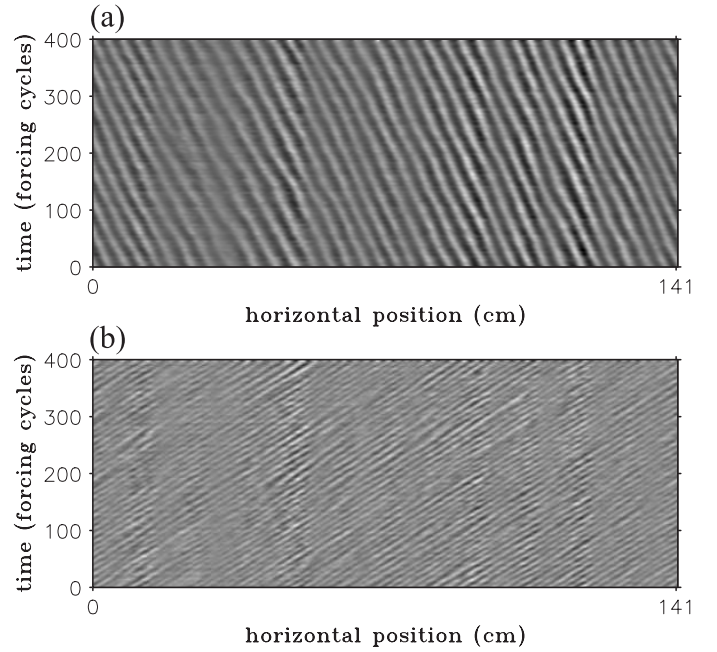


Figure 4. Space time plot showing the brightness of the granular surface at maximum wave amplitude every other forcing cycle for $\Gamma = 2.84$ (a) and $\Gamma = 4.22$ (b).

crossover frequency $f_{\text{gm}} = v_{\text{gm}}/2\pi a$. Plugging in our values for d and a , we obtain $f_{\text{gm}} = 34 \text{ Hz}$, which is well above the frequencies at which we do our measurements. So we conclude that the surface waves examined here are not caused by a horizontal back and forth motion of the particles, but by either a bending of the layer or a spatial density modulation. In fact although the particles of the top layer are fluidised and perform jumps their movement seems to be random in character and not coupled to the wave motion. Also the dependence of the wavelength on Γ reported here is consistent with the results of Metcalf et al. (1997) in the immobile grain regime. Evidence for a saturation of the wavelength at high Γ in the immobile grain regime has been given by Clément et al. (1996). They found the wavelength to be constant over a wide range of f and Γ , taking on a value of about twice the layer depth, which is in reasonable accord with what we obtain from our model fit.

The space-time-plots of Figures 4a, b display the surface brightness at maximum amplitude on every other cycle, accelerations Γ being 2.84 and 4.22, respectively. They demonstrate that we are actually dealing with a drifting standing wave. The wave pattern is not exactly at the same position after two forcing cycles, but shifted a little to one or the other direction, depending on Γ . To obtain the drift velocity, the real space brightness data are Fourier transformed and the phase of the wave number belonging to the dominant wavelength is tracked. From the rate of phase change one is able to calculate the velocity of the pattern movement. Results are plotted in Figure 5 and compared to velocity measurements for a tracer particle that indicates the velocity of the surrounding material. As tracer particle serves a coloured glass bead with a diameter of 6 mm, which is sufficiently large

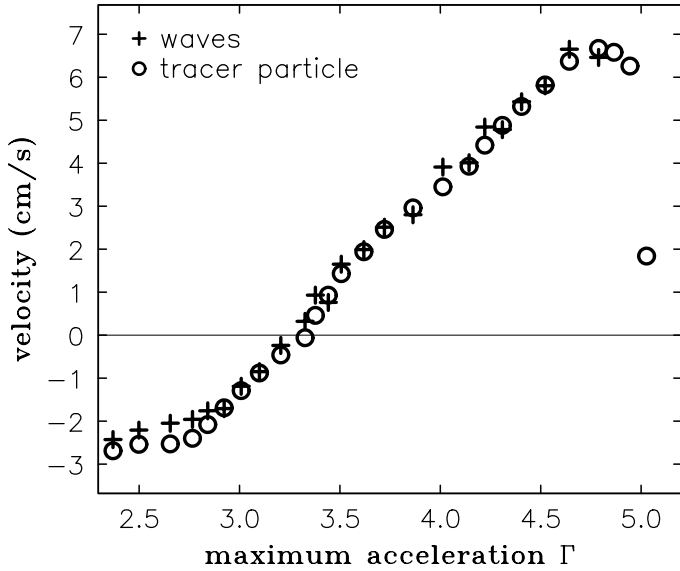


Figure 5. Measured velocity of a tracer particle (circles) and drift velocity of the surface waves (crosses) over the normalized acceleration Γ . Throughout the measurement the driving amplitude was kept constant at 1.47 mm.

to prevent it from submerging, so that it remains visible all of the time. The drift velocity of the surface wave and the transport velocity of the granular material coincide. Worth mentioning is the fact that the surface waves disappear at the same value of Γ where the transport velocity starts to decrease.

4 CONCLUSIONS

In the framework of our investigations into the phenomenon of granular surface waves upon circular oscillation of the container, we measured the wavelength dependence on the forcing acceleration Γ in the regime of low horizontal grain mobility. A drift of the standing wave pattern was found to occur, and the drift velocity matches the transport velocity of the granular material. Both velocities strongly depend on the forcing acceleration and even reverse sign at $\Gamma \approx 3.3$. The detected waves are similar to those seen in containers oscillating purely in the vertical direction. Obviously the horizontal oscillation component has little influence on the wave phenomenon, except for the drift.

Future experiments will be carried out in a transparent container. This will uncover the shape of the lower boundary of the layer during the flight phase. For a bending wave we would expect arches underneath peaks of the surface undulations. Furthermore one could monitor the fluidisation state of the granular bed at different heights in the course of time.

Finally a detailed characterization of the surface wave phenomenon in vibrated granular layers will provide data for tests of continuum models of granular matter. Of some practical interest for industrial applications are the mixing properties in the surface wave regime. One might expect enhanced self diffusion in the presence of an undulated surface, compared to the state with a flat surface at lower and higher acceleration Γ .

We thank Rafał Grochowski and Peter Walzel for the construction of the vibratory conveyor and Hamid El hor and Stefan Linz for valuable discussions. This work was supported by Deutsche Forschungsgemeinschaft as part of the program "Verhalten granularer Medien".

REFERENCES

- Clément, E., Vanel, L., Rajchenbach, J., & Duran, J. 1996. Pattern formation in a vibrated granular layer. *Phys. Rev. E* 53: 2972–2975.
- Grochowski, R., Walzel, P., Rouijaa, M., Kruelle, C. A., & Rehberg, I. 2004. Reversing granular flow on a vibratory conveyor. *Appl. Phys. Lett.* 84: 1019–1021.
- Jähne, B. 2002. *Digital image processing*. Berlin: Springer.
- Melo, F., Umbanhowar, P., & Swinney, H. L. 1994. Transitions to parametric wave patterns in a vertically oscillated granular layer. *Phys. Rev. Lett.* 72: 172–175.
- Melo, F., Umbanhowar, P., & Swinney, H. L. 1995. Hexagons, kinks, and disorder in oscillated granular layers. *Phys. Rev. Lett.* 75: 3838–3841.
- Metcalf, T. H., Knight, J. B., & Jaeger, H. M. 1997. Standing wave patterns in shallow beds of vibrated granular material. *Physica A* 236: 202–210.
- Rouijaa, M., Kruelle, C. A., Rehberg, I., Grochowski, R., & Walzel, P. 2005. Transport and pattern formation in granular materials on a vibratory conveyor. *Chem. Eng. Technol.* 28: 41–44.
- Umbanhowar, P. & Swinney, H. L. 2000. Wavelength scaling and square/stripe and grain mobility transitions in vertically oscillated granular layers. *Physica A* 288: 344–362.
- Wassgren, C. R., Hunt, M. L., & Brennen, C. E. 1997. Investigation of $f/2$ and $f/4$ waves in granular beds subject to vertical, sinusoidal oscillations. In R. P. Behringer & J. T. Jenkins (eds), *Powders & Grains 97*: Rotterdam: 433–436. Balkema.